TITLE: Longitudinal Profiling of the Intestinal Microbiome in Children with Cystic Fibrosis Treated with Elexacaftor-Tezacaftor-Ivacaftor

WORD COUNT (MAIN TEXT): 3519

AUTHORS: Seth A. Reasoner[1]*, Rachel Bernard[2]*, Adam Waalkes[3], Kelsi Penewit[3], Janessa Lewis[3], Andrew G. Sokolow[4], Rebekah F. Brown[4], Kathryn M. Edwards[5], Stephen J. Salipante[3], Maria Hadjifrangiskou[1,6,7], Maribeth R. Nicholson[2,7]

AFFILIATIONS:
1. Division of Molecular Pathogenesis, Department of Pathology, Microbiology & Immunology, Vanderbilt University Medical Center, Nashville, TN, USA
2. Division of Gastroenterology, Hepatology, and Nutrition, Department of Pediatrics, Monroe Carrell Junior Children's Hospital at Vanderbilt, Nashville, TN, USA
3. Department of Laboratory Medicine and Pathology, University of Washington, Seattle, WA, USA
4. Division of Allergy, and Immunology, and Pulmonary Medicine, Department of Pediatrics, Monroe Carrell Junior Children's Hospital at Vanderbilt, Nashville, TN, USA
5. Division of Infectious Diseases, Department of Pediatrics, Monroe Carrell Junior Children's Hospital at Vanderbilt, Nashville, Tennessee, USA
6. Center for Personalized Microbiology (CPMi), Vanderbilt University Medical Center, Nashville, TN, USA
7. Vanderbilt Institute for Infection, Immunology and Inflammation, Vanderbilt University Medical Center, Nashville, Tennessee, USA

**These authors contributed equally to this work*

Corresponding Author:
Maribeth R. Nicholson, MD, MPH
Monroe Carell Jr. Children's Hospital at Vanderbilt
2200 Children's Way, Nashville, TN 37232
Telephone: +1 615 322 7449
E-mail: maribeth.r.nicholson@vumc.org

KEY WORDS
Cystic fibrosis; CFTR modulators; microbiome; elexacaftor; ivacaftor; tezacaftor; metagenomic sequencing; intestinal inflammation; antibiotic resistance; pediatric

ABSTRACT

The intestinal microbiome influences growth and disease progression in children with cystic fibrosis (CF). Elexacaftor-tezacaftor-ivacaftor (ELX/TEZ/IVA), the newest pharmaceutical modulator for CF, restores function of the pathogenic mutated CFTR channel. We performed a single-center longitudinal analysis of the effect of ELX/TEZ/IVA on the intestinal microbiome, intestinal inflammation, and clinical parameters in children with CF. Following ELX/TEZ/IVA, children with CF had significant improvements in BMI, $ppFEV_1$ and required fewer antibiotics for respiratory infections. Intestinal microbiome diversity increased following ELX/TEZ/IVA coupled with a decrease in the intestinal carriage of *Staphylococcus aureus*, the predominant respiratory pathogen in children with CF. There was a reduced abundance of microbiome-encoded antibiotic-resistance genes. Microbial pathways for aerobic respiration were reduced after ELX/TEZ/IVA. The abundance of microbial acid tolerance genes was reduced, indicating microbial adaptation to increased CFTR function. In all, this study represents the first comprehensive analysis of the intestinal microbiome in children with CF receiving ELX/TEZ/IVA.

1. INTRODUCTION

Cystic fibrosis (CF) is an autosomal recessive disease affecting a total of 40,000 individuals in the United States[1]. CF is caused by mutations in the CF transmembrane conductance regulator (*CFTR*) gene resulting in decreased epithelial transport of chloride and bicarbonate ions. These mutations result in mucus obstruction which presents with severe multi-organ dysfunction, principally affecting the airways and gastrointestinal tract[2–5]. The gastrointestinal complications include malnutrition, dysmotility, and hepatopancreaticobiliary disease[2]. The CF intestinal microbiome is characterized by presence of respiratory pathogens, such as *Staphylococcus aureus*, and an inflammatory intestinal phenotype, as exemplified by higher rates of inflammatory bowel disease (IBD) and colon cancer among people with CF[6–11]. Importantly, nutritional status and intestinal dysbiosis in children with CF have been linked to growth failure, disease progression, and risk of future lung transplantation[12–16].

Over the past decade small molecule therapies which address the primary defect in the CFTR protein and rescue CFTR function in select genotypes have been developed. These "CFTR modulators" have dramatically changed the trajectory of CF patient care, yielding remarkable improvements in lung function, growth, and projected lifespan[17]. The most recent CFTR modulator formulation approved for clinical care, elexacaftor-tezacaftor-ivacaftor (ELX/TEZ/IVA), includes two CFTR correctors (ELX & IVA) and one CFTR potentiator (TEZ)[18].

The approval of ELX/TEZ/IVA is anticipated to be the most important advancement in CF therapy since *CFTR* was identified over 30 years ago[17,18].

Given the progressive nature of CF, initiation of therapy in early childhood is critical to stall disease progression. ELX/TEZ/IVA was approved by the FDA for pediatric patients in 2019 (ages 12 years and older) and 2021 (ages 6-11 years old). The impact of ELX/TEZ/IVA on clinical outcomes and the intestinal microbiome in children with CF requires targeted study. To date, studies examining the effects of CFTR modulators on the intestinal microbiome have been limited by the use of single modulator formulations or small cohort sizes[19–21]. Importantly, no studies have characterized the effect of ELX/TEZ/IVA on the intestinal microbiome of children with CF. We therefore undertook a longitudinal study to identify changes in clinical outcomes and the intestinal microbiomes of pediatric patients following the initiation of ELX/TEZ/IVA. To our knowledge, this study represents the first comprehensive study of the highly effective CFTR modulator formulation ELX/TEZ/IVA on the intestinal microbiome of children with CF.

2. METHODS

2.1 Recruitment of Subjects

Pediatric patients with a diagnosis of CF at Monroe Carell Jr. Children's Hospital at Vanderbilt (MCJCHV) were recruited beginning in July 2017 with follow-up until October 2022. Patients with the Phe508 CFTR mutation who were deemed eligible for ELX/TEZ/IVA by their pulmonologist were eligible for this study. Patients previously treated with other CFTR modulator regimens were permitted. Patients with pre-existing non-CF gastrointestinal disease were excluded. A total of 39 participants were recruited (Table 1). Informed consent was obtained from parental guardians, and assent was obtained from pediatric subjects in accordance with institutional research ethics guidelines. This study was approved by the MCJCHV Institutional Review Board (IRB # 200396). The lead investigators of this study had no direct role in the patients' routine medical care. All study data were stored in a Research Electronic Data Capture (REDCap) database per institutional guidelines[22].

2.2 Study Timepoints

Our analysis included stool samples from up to four timepoints per patient: two timepoints before ELX treatment (T1 & T2) and two timepoints after initiating ELX/TEZ/IVA (T3 & T4) (Figure 1B). For clinical outcomes, data was either analyzed by individual timepoints (T1-T4) or time points were combined for pre-ELX/TEZ/IVA samples (T1 & T2 combined) and post-ELX-TEZ/IVA samples (T3 & T4 combined). Analysis of individual timepoints permitted assessment

of additional differences between the 6 to 12-month periods after ELX/TEZ/IVA initiation. For microbiome comparisons, analysis was based on combined pre-ELX/TEZ/IVA samples (T1 & T2) and post-ELX-TEZ/IVA samples (T3 & T4).

2.3 Stool Sample Collection and DNA Extraction

Stool samples were collected prior to ELX/TEZ/IVA initiation, either through targeted collection as part of this study or from our center's biobank of CF stool samples[23,24]. Subsequent stool samples were collected at approximately 6- and 12-month intervals after initiation of ELX/TEZ/IVA (Figure 1A). Fecal samples were collected in sterile collection cups and refrigerated until transport to the laboratory. Patients who were unable to provide a stool sample in clinic were provided with an OMNIgene®•GUT stool collection kit for at home collection and stabilization, returned via overnight shipping, and stored according to manufacturer specifications. Aliquots of stool samples were aseptically aliquoted into cryovials in a laminar flow biosafety cabinet to minimize aerosols and stored at -80ºC until processing. Percent predicted forced expiratory volume in one second ($ppFEV_1$) values were obtained in the outpatient setting at the time of stool sample collection; the highest spirometry value of three attempts was recorded. Clinical data including body mass index (BMI, percentiles), percentage predicted forced expiratory volume in 1 second ($ppFEV_1$), medications, and laboratory values were recorded for visits when a stool sample was collected. Total DNA was extracted from 114 stool samples using QIAamp PowerFecal Pro DNA Kits according to the manufacturer's instructions. Bead beating for efficient lysis was conducted for 10 minutes. All steps, excluding bead beating and centrifugation, were conducted in a laminar flow biosafety cabinet. No human DNA depletion or enrichment of microbial DNA was performed. DNA yield was estimated by spectrophotometry (NanoDrop™2000c) in parallel with ensuring satisfactory A260/A280 ratio for DNA purity.

2.4 Fecal Calprotectin Measurements

Fecal calprotectin was measured using the Calprotectin ELISA Assay Kit (Eagle Biosciences). Duplicate portions of stool (50-100mg) were weighed and processed according to the manufacturer's instructions. Absorbance was measured with a SpectraMax® i3x (Molecular Devices). Fecal calprotectin (µg/g feces) was calculated using a 7-point standard curve. The assay's reported normal cut-off is <43.2 µg/g.

2.5 Shotgun Metagenomic Sequencing

Sequencing libraries were prepared using Illumina® reagents as described elsewhere[25]. Pooled libraries were sequenced on NextSeq2000 to generate 150-bp paired-end reads. An average of 13.9 million reads were produced per sample (range 9.1 to 30.1 million). Sequencing adaptors and low-quality sequences were trimmed with fastq-mcf from ea-utils-1.1.2.779[26].

2.6 Taxonomic and Functional Profiling of Metagenomic Sequence Data

Species abundances were determined with MetaPhlAn4 following read alignment to the MetaPhlan4 database[27]. Diversity metrics were calculated with the vegan R package[28] and plotted with ggplot2. A weighted UniFrac distance matrix was constructed with the MetaPhlAn R script "calculate_unifrac". Functional profiling was conducted with HUMAnN 3.0 with mapping to UniRef90 gene-families and MetaCyc metabolic pathways[29–31]. UniRef90 gene-families were reformatted into KEGG orthology (KO) groups using the HUMAnN command "humann_regroup_table". In total, we identified 722 species, 526 MetaCyc pathways, and 8634 distinct KO groups annotations in the 114 samples. All functional annotations were normalized using the HUMAnN command "humann_renorm_table --units cpm". Antibiotic resistance genes were identified by ShortBRED[32] with the reference Comprehensive Antibiotic Resistance Database (CARD version 2017)[33]. ARG abundance was calculated as reads per kilobase of reference sequence per million sample reads (RPKM).

2.7 Microbial Dysbiosis Index

The Microbial Dysbiosis Index was calculated as the log10 of the ratio of the relative abundance of taxa which were previously positively and negatively associated with newly diagnosed pediatric Crohn's disease[34]. Specifically, the numerator includes *Enterobacteriaceae*, *Pasteurellaceae*, *Fusobacteriaceae*, *Neisseriaceae*, *Veillonellaceae*, *Gemellaceae*; the denominator includes *Bacteroidales*, *Clostridiales* (excluding *Veillonellaceae*), *Erysipelotrichaceae*, and *Bifidobacteriaceae*. The microbial dysbiosis index has been previously applied to stool samples of children with CF[35,36].

2.8 Differential Abundance Testing

We used MaAsLin2 (Microbiome Multivariable Associations with Linear Models, Maaslin2 R package) to identify differentially abundant features[37]. We included ELX/TEZ/IVA, age, and recent antibiotic exposure as fixed effects. Subject ID was specified as a random effect due to multiple samples from the same subject. Species, KEGG orthologs, and MetaCyc pathways detected at least 10% of samples were tested (i.e., prevalence = 0.1); no minimum abundance

was specified. Abundances were log transformed within the MaAsLin2 function. The general linear “LM” model was used. MaAsLin2 coefficients are equivalent to log2(FoldChange). The Benjamini-Hochberg procedure was used to correct P values, and corrected P values are reported as False Discovery Rates (FDR).

2.9 Statistical Analyses

Statistical analyses were conducted using GraphPad Prism 9 and R (version 4.2.1) software. Details of the statistical tests used and the significance thresholds are presented in the figure legends. All box-plot graphs are defined as: center line—median; box limits—upper and lower quartiles; whiskers—1.5× interquartile range.

2.10 Reproducibility and Data Availability

The results can be reproduced using raw sequence data that are available on NCBI-Genbank databases under Bioproject PRJNA948536 or using processed data in the Supplementary Dataset 1. Bioinformatic code is available within the repository https://github.com/reaset41/CF-GI-Microbiome-ELX-TEZ-IVA.

3. RESULTS

3.1 Study Cohort and Stool Sample Collection

Stool samples were collected from a total of 39 children with CF (Table 1). The median (IQR) age of participants at the time of ELX/TEZ/IVA initiation was 9.86 years old (8.87, 12.15) and 53.4% were male. Of these, 35.9% (14/39) had CFTR modulator use before ELX/TEZ/IVA. Patients provided an average of 2.92 stool samples with all patients providing at least one stool sample prior to starting ELX/TEZ/IVA (T1 median= 33.6 months before ELX/TEZ/IVA initiation, IQR 28.6, 36.7 months and T2 median=0.64 months before ELX/TEZ/IVA initiation, IQR 0.13, 2.2 months). Subsequent stool samples were collected at approximately 6- and 12-month intervals (T3 median=5.97 months, IQR 5.38, 6.92 months and T4 median=12.39 months, IQR 11.1, 13.1 months). There was a total of 114 stool samples with 53 samples before ELX/TEZ/IVA therapy and 61 samples after ELX/TEZ/IVA treatment.

3.2 Clinical Improvement after ELX/TEZ/IVA

To determine our cohort’s clinical response to ELX/TEZ/IVA, we compared clinical metrics from before and after ELX/TEZ/IVA initiation. Both BMI percentile and $ppFEV_1$ increased in the timepoints after ELX/TEZ/IVA compared to pre-ELX/TEZ/IVA timepoints (Figure 1C-D &

S1A-B). Median BMI percentile increased from the 54th percentile to the 67th percentile after ELX/TEZ/IVA (Figure 1D). Likewise, there was a mean change in $ppFEV_1$ of 12.3 percentage points (95% CI 6.7-17.8) before and after ELX/TEZ/IVA (Figure 1C). Between 6- and 12-months after ELX/TEZ/IVA, there was no further significant improvement in either BMI or $ppFEV_1$ (Figure S1A-B, T3 & T4). Consistent with increased BMI, weight percentile increased after ELX/TEZ/IVA (Figure S1C). Height percentile increased between T2 and both T3 and T4 (Figure S1D, P=0.013, P=0.026, respectively), though not between T1 and T3 & T4. Total antibiotic days per patient were aggregated and decreased from a median of 22.5 days per 6-months before ELX/TEZ/IVA to 0 antibiotic days per 6-months after ELX/TEZ/IVA (Figure 1E, P<0.0001).

3.3 Microbiome Diversity Increases After ELX/TEZ/IVA

From shotgun metagenomic sequencing on 114 stool samples, we compared measures of microbiome diversity. Alpha diversity, as measured by the Shannon index and richness (observed species), significantly increased following ELX/TEZ/IVA (Figures 2A-B, P=0.021 and P=0.026, respectively). The number of species observed increased from a median (IQR) of 83 (62, 115) species before ELX/TEZ/IVA to 109 (82,125) species after ELX/TEZ/IVA (Figure 2B). The cumulative increases in alpha diversity were not significantly different when comparing between the four timepoints individually (Figures S2A-B), and there were no differences in overall community composition (beta-diversity) before and after ELX/TEZ/IVA (Figures S2C-D).

To determine the influence of antibiotic exposure on microbiome diversity measures regardless of ELX/TEZ/IVA status, we categorized patient stool samples as having received antibiotics within the six-months prior to stool sample collection (n=62) or no antibiotic receipt (n=52). Recent antibiotic exposure significantly impacted alpha diversity measures reducing Shannon diversity and richness (Figures 2C-D). Likewise, population structure (beta-diversity) was significantly different between samples with and without recent antibiotic exposure (Figure S2E, permutational multivariate analysis of variance [PERMANOVA]=0.003).

3.4 Microbiome Encoded Antibiotic Resistance Genes Decrease After ELX/TEZ/IVA

As discussed above, patients required far fewer antibiotics after starting ELX/TEZ/IVA (Figure 1E & S3A). Since the intestinal microbiome is a reservoir of antibiotic resistant genes (ARGs)[38], we compared the number and type of intestinal ARGs before and after ELX/TEZ/IVA initiation. Across the 114 samples, we detected a total of 309 unique ARGs. The median number of unique ARGs nominally decreased from a median 86 ARGs (IQR 40, 96) before

ELX/TEZ/IVA to a median 68 ARGs (IQR 38, 90) after ELX/TEZ/IVA (Figure S3B, P=0.31). ARG abundance decreased from a median of 1180 RPKM (IQR 815.4, 1761.1) to 829 RPKM (IQR 460.5, 1299.0) (Figure 2E, P=0.0097) though this effect was likely mediated by reduced antibiotic use.

Next, we aggregated the relative abundance of ARGs by antibiotic class to which they confer resistance (Figure 2F). The abundance of ARGs conferring resistance to peptide antibiotics and ungrouped antibiotics ("Other") significantly decreased after ELX/TEZ/IVA (Figures 2E & S3C-E, P=0.012, P=0.022 respectively). The most prevalent antibiotics within the peptide ARG class included *arnA* (n=72/114), *yojI* (n=71/114), *pmrF* (n=74/114) and *pmrC* (n=71/114). *arnA, pmrF* and *pmrC* modify Lipid A on bacterial cells to repel cationic peptide antibiotics, whereas *yojI* is a peptide efflux pump. The most prevalent ARGs within the "Other" group were *fabI* (n=84/114), *gadE* (78/114), and EF-Tu mutations (n=75/114). These ARGs or mutations confer resistance to isoniazid/disinfecting agents (*fabI*), acid resistance and efflux pump (*gadE*), and elfamycin (EF-Tu). Despite being the most prevalent, none of these ARGs were independently altered in abundance following ELX/TEZ/IVA (Figures S3D & S3F).

3.5 Alterations to Specific Bacterial Taxa Following ELX/TEZ/IVA

To determine whether specific bacterial taxa change following ELX/TEZ/IVA treatment, we used MaAsLin2 (Microbiome Multivariable Associations with Linear Models) to identify differentially abundant microbial species[37]. Seventeen species were differentially abundant between samples before and after ELX/TEZ/IVA (FDR<0.1, Figure 3A and Table S3), with eleven species increasing in abundance after ELX/TEZ/IVA, and six species decreasing. The three species with the lowest FDR and, therefore, highest reliability were *Butyricicoccus* SGB14985, *S. aureus,* and *Roseburia faecis* (Figure 3A-B). *Butyricicoccus* SGB14985, an uncultivated species, was decreased in abundance following ELX/TEZ/IVA (fold change 0.16, FDR=0.022). *Roseburia faecis* was increased in abundance following ELX/TEZ/IVA (fold change 7.35, FDR=0.025) and negatively correlated with recent antibiotic exposure (Figure S4A, fold change 0.20, FDR=0.086). Since the intestinal tract is a reservoir for respiratory pathogens in people with CF[10,39,40], we performed focused analysis of CF pathogens. *S. aureus*, the predominant respiratory pathogen in children with CF[41], was decreased in abundance after ELX/TEZ/IVA (Figure 3A-B, fold change 0.40, FDR=0.042). *Pseudomonas aeruginosa*, an additional respiratory pathogen of importance in CF, was detected in only two of the 114 stool samples. Other members of the respiratory microbiota which are frequently detected in the

intestines[10,36]—specifically the genera *Haemophilus*, *Prevotella*, *Streptococcus*, *Veillonella*—did not significantly change after ELX/TEZ/IVA initiation (Figure S4B).

3.6 Intestinal Inflammation Decreases After ELX/TEZ/IVA

Fecal calprotectin was measured across the four timepoints and markedly decreased following ELX/TEZ/IVA (Figures 4A & S5A). Overall, mean fecal calprotectin decreased from 109 µg/g before ELX/TEZ/IVA to 44.8 µg/g for a mean decrease of 64.2 µg/g (95% CI -16.1, -112.3, Figure 4A). We then computed the microbial dysbiosis index[34] and noted a nominal reduction in the microbial dysbiosis index following ELX/TEZ/IVA (Figure 4B, P=0.068), which was less pronounced when comparing samples from patients with recent antibiotic exposure and those without (Figure 4C, P=0.77).

3.7 Microbiome Functional Changes Reveal Specific Disease-Relevant Changes

From the 114 stool samples, alignment of sequencing reads to known microbial proteins and pathways identified 8634 KEGG orthology (KO) protein groups and 526 MetaCyc metabolic pathways, consistent with prior studies of the intestinal microbiota[42]. There were 249 KO groups differentially abundant with respect to ELX/TEZ/IVA use (MaAsLin2 FDR<0.25, Figure 4D & Table S6). Strikingly, a common thread among differentially abundant KO groups was a decreased abundance of genes encoding oxidative phosphorylation functions following ELX/TEZ/IVA (Figure 4D). Seven of the top 10 most differentially abundant KO groups were components of the electron transport chain (Figures 4D & S5B and Table S7) and included NADH-ubiquinone oxidoreductases (e.g., K03883, K03881, K03884, & K03880), F-type ATPase subunits (e.g., K02125), and cytochrome c oxidase subunits (e.g., K02262, K02261, & K02256). The taxa contributing to oxidative phosphorylation KO groups were not consistently annotated (Figure S5C). This indicates that a specific taxonomic signature was not responsible for the reduced abundance of oxidative phosphorylation KO groups (Figure 5SC). These results were corroborated by MaAsLin2 differential abundance testing of MetaCyc pathways. Sixty-four MetaCyc pathways were differentially abundant with respect to ELX/TEZ/IVA use (MaAsLin2 FDR<0.25, Figure 4E & Table S9). Two of these pathways corresponded to aerobic respiration (PWY-3781 and PWY-7279). Furthermore, 13 amino acid biosynthesis pathways were universally prevalent in all stool samples (114/114) and significantly increased in abundance following ELX/TEZ/IVA (Figure 4E, FDDR<0.25). This indicates increased biosynthetic capacity of the intestinal microbiome following ELX/TEZ/IVA.

Another intriguing observation was the reduced abundance of KO groups involved in acid tolerance and transport following ELX/TEZ/IVA (Figure 4D). KO groups involved in organic acid transport (e.g., K03290 & K23016) and proton-symporters (e.g., K11102 & K03459) were reduced in abundance following ELX/TEZ/IVA. Likewise, an acidity-responsive transcriptional regulator (K03765, *cadC*) was decreased in abundance following ELX/TEZ/IVA (Figure 4D and Table S7, fold change 0.42, FDR=0.27).

4. DISCUSSION

ELX/TEZ/IVA has changed the trajectory of CF patient care and dramatically improved clinical outcomes. Nutritional status and intestinal dysbiosis are strong predictors of future clinical outcomes, particularly in children with CF[12–14]. We therefore sought to determine the effects of ELX/TEZ/IVA on intestinal inflammation and the intestinal microbiome in children with CF. Herein, we present a comprehensive longitudinal characterization of the intestinal microbiome in children with CF treated with ELX/TEZ/IVA. We identified widespread changes to the intestinal microbiome after ELX/TEZ/IVA including taxonomic composition, reduced carriage of ARGs, and altered microbiota metabolic functions.

Although randomized controlled trials demonstrated that ELX/TEZ/IVA was safe and effective, there are limited post-approval clinical data, particularly in children ages 6-11 years[43–47]. BMI and $ppFEV_1$ are useful markers of clinical response to CFTR modulator treatment in children[48]. Our cohort strongly supported prior observations with improvements in $ppFEV_1$ and BMI percentile within six-months of starting ELX/TEZ/IVA, with no differences at later time points. Furthermore, between the timepoint immediately before ELX/TEZ/IVA initiation (T2) and post-ELX/TEZ/IVA timepoints (T3 & T4), there was a significant increase in height percentile (Figure S1D). This suggests that CFTR modulator therapy may improve linear growth failure of children with CF. In sum, these results support the clinical responsiveness of children with CF to ELX/TEZ/IVA.

The gastrointestinal microbiome influences whole-body physiology. CF intestinal dysbiosis begins in infancy, diverging from healthy controls by 1-year of age[10,14,36,49–51]. Intriguingly, the microbiome of people with CF resembles that of patients with IBD, a group with a dysbiotic intestinal microbiome[35,52,53]. In children with CF, markers of intestinal inflammation correlate with growth failure[54,55]. Moreover, intestinal inflammation in people with CF is linked to higher rates of IBD and colorectal cancer in people with CF[6,7,56]. Fecal calprotectin, a laboratory marker of intestinal inflammation[57–59], significantly decreased following ELX/TEZ/IVA (Figure 4A), corroborating a prior report in the pediatric PROMISE cohort[60]. Using a dysbiosis index of

bacterial taxa correlated with pediatric Crohn's disease[34], we identified that dysbiosis nominally decreased following ELX/TEZ/IVA initiation (Figure 4B). At the species level, the butyrate-producing species *Roseburia faecis* was significantly enriched following ELX/TEZ/IVA (Figure 3A-B). Prior studies have identified *R. faecis* as reduced in abundance in people with CF[11,61–63]. In parallel, we detected reduced abundance of genes involved in oxygen-dependent metabolism following ELX/TEZ/IVA (Figures 4D-E). Intestinal inflammation is characterized by a shift towards oxygen-dependent microbiota metabolism, perpetuating a cycle of inflammatory damage[64–66]. From multiple lines of evidence, our results suggest that ELX/TEZ/IVA reduces intestinal inflammation in children with CF.

Respiratory infections require frequent antibiotics in people with CF. Some respiratory pathogens also colonize the intestinal tract and temporally correlate with respiratory infections[10,39,40]. *S. aureus* is among the first pathogens to colonize the respiratory tract and cause infections in children with CF[41]. We detected reduced intestinal abundance of *S. aureus* following ELX/TEZ/IVA (Figures 3A-B). Antibiotic exposure in people with CF has been associated with increased intestinal carriage of antibiotic resistant bacteria which are a poor prognostic factor[67,68]. Following ELX/TEZ/IVA, patients in our cohort required far fewer antibiotics (Figure 1E). In turn, we detected reduced intestinal abundance of ARGs (Figure 2E). These results indicate disease-relevant taxonomic changes to the intestinal microbiome following ELX/TEZ/IVA, as well as reduced ARGs.

The CFTR channel permits transepithelial movement of bicarbonate ($HCO3^-$) and chloride (Cl^-)[5]. Intestinal pH is lower in people with CF due to the lack of neutralizing bicarbonate[69] yet increases with CFTR modulator treatment, consistent with increased CFTR activity in the intestinal tract[70]. We observed a reduced abundance of microbial protein groups associated with acid tolerance (Figure 4D), consistent with microbial adaptation to increased CFTR channel function in the intestines. These results display physiologically intuitive functional changes to the microbiome post-ELX/TEZ/IVA.

Our study is strengthened by longitudinal sampling over a five-year period combined with the real-world use of ELX/TEZ/IVA. Using shotgun metagenomic sequencing, we comprehensively compared microbiota differences before and after ELX/TEZ/IVA. Although our study was limited by the single-center focus, our cohort mirrors the overall CF pediatric population in clinical and demographic factors (Table 1). Sampling of the intestinal microbiome over extended periods will be important to uncover additional long-term improvements to the microbiome.

In summary, our results indicate that the CFTR modulator ELX/TEZ/IVA improves widespread dysbiosis in the intestinal microbiome of children with CF. We identified taxonomic and functional changes to the intestinal microbiome that represent improvements to CF intestinal dysbiosis. Our results also support that CFTR modulators reduce intestinal inflammation in children with CF.

AUTHOR CONTRIBUTIONS (CRediT author statement)

SAR: Investigation, Methodology, Data Curation, Formal analysis, Writing - Original Draft
RB: Conceptualization, Funding Acquisition, Investigation, Data Curation, Writing - Original Draft
AW: Investigation, Software
KP: Investigation
JS: Investigation
AGS: Supervision, Writing - Review & Editing
RFB: Supervision, Writing - Review & Editing
KME: Supervision, Writing - Review & Editing
SJS: Investigation, Data Curation, Software, Writing - Review & Editing
MH: Supervision, Writing - Review & Editing
MRN: Conceptualization, Funding Acquisition, Investigation, Supervision, Writing - Original Draft

ACKNOWLEDGEMENTS AND FUNDING

We would like to express our sincere appreciation to the patients and their families who enthusiastically participated in this study. We would like to thank our advanced practitioner and nursing colleagues from the Pediatric Pulmonology clinic at the Monroe Carrell Jr. Children's Hospital at Vanderbilt for their collegiality and assistance with this study. This work was supported, in part, by National Institutes of Health (NIH) grants T32DK007673 (RB), K23AI156132 (MRN), F30AI169748 (SAR), T32GM007347 (SAR), and P30DK089507 (SJS); the Cystic Fibrosis Foundation (SINGH19R0 to SJS) and the Thrasher Research Fund (RB and MRN).

CONFLICTS OF INTERESTS

All authors declare that they have no conflicts of interest relevant to this work.

DATA AVAILABILITY

All sequence data derived from this work are publicly available in NCBI-Genbank databases under Bioproject PRJNA948536. All processed data and code used for bioinformatic analysis is available within the repository: https://github.com/reaset41/CF-GI-Microbiome-ELX-TEZ-IVA.

AUTHOR ORCID IDs:
SAR: 0000-0002-7791-1641
RB: 0000-0002-6689-5658
AW: 0000-0002-5202-1108
KP: 0000-0003-1454-6381
AGS: 0000-0002-5495-1237
RFB: 0000-0003-3632-4587
KME: 0000-0003-3912-9832
SJS: 0000-0001-8355-6992
MH: 0000-0003-4249-8997
MRN: 0000-0003-3941-5599

REFERENCES

1. CF Foundation Estimates Increase in CF Population (2022). Cystic Fibrosis Foundation. https://www.cff.org/news/2022-07/cf-foundation-estimates-increase-cf-population.
2. Moshiree, B., Freeman, A.J., Vu, P.T., Khan, U., Ufret-Vincenty, C., Heltshe, S.L., Goss, C.H., Schwarzenberg, S.J., Freedman, S.D., Borowitz, D., et al. (2022). Multicenter prospective study showing a high gastrointestinal symptom burden in cystic fibrosis. Journal of Cystic Fibrosis. 10.1016/j.jcf.2022.10.006.
3. De Lisle, R.C., and Borowitz, D. (2013). The cystic fibrosis intestine. Cold Spring Harb Perspect Med *3*, 1–18. 10.1101/cshperspect.a009753.
4. Kreda, S.M., Davis, C.W., and Rose, M.C. (2012). CFTR, mucins, and mucus obstruction in cystic fibrosis. Cold Spring Harb Perspect Med *2*. 10.1101/cshperspect.a009589.
5. Elborn, J.S. (2016). Cystic fibrosis. The Lancet *388*, 2519–2531. 10.1016/S0140-6736(16)00576-6.
6. Hadjiliadis, D., Khoruts, A., Zauber, A.G., Hempstead, S.E., Maisonneuve, P., Lowenfels, A.B., Braid, A.L., Cullina, J., Daggett, A., Fink, A., et al. (2018). Cystic Fibrosis Colorectal Cancer Screening Consensus Recommendations. Gastroenterology *154*, 736-745.e14. 10.1053/j.gastro.2017.12.012.
7. Hegagi, M., Aaron, S.D., James, P., Goel, R., and Chatterjee, A. (2017). Increased prevalence of colonic adenomas in patients with cystic fibrosis. Journal of Cystic Fibrosis *16*, 759–762. 10.1016/j.jcf.2017.07.009.
8. Schwarzenberg, S.J., Wielinski, C.L., Shamieh, I., Carpenter, B.L.M., Jessurun, J., Weisdorf, S.A., Warwick, W.J., and Sharp, H.L. (1995). Cystic fibrosis-associated colitis and fibrosing colonopathy. J Pediatr *127*, 565–570. 10.1016/S0022-3476(95)70113-3.
9. Burton, S., Hachem, C., and Abraham, J. (2021). Luminal Gastrointestinal Manifestations of Cystic Fibrosis. Curr Gastroenterol Rep *23*. 10.1097/00219246-200124060-00001.
10. Madan, J.C., Koestle, D.C., Stanton, B.A., Davidson, L., Moulton, L.A., Housman, M.L., Moore, J.H., Guill, M.F., Morrison, H.G., Sogin, M.L., et al. (2012). Serial analysis of the gut and respiratory microbiome in cystic fibrosis in infancy: Interaction between intestinal

and respiratory tracts and impact of nutritional exposures. mBio *3*. 10.1128/mBio.00251-12.

11. Price, C.E., and O'Toole, G.A. (2021). The gut-lung axis in cystic Fibrosis. J Bacteriol *203*. 10.1128/JB.00311-21.

12. Steinkamp, G., and Wiedemann, B. (2002). Relationship between nutritional status and lung function in cystic fibrosis: Cross sectional and longitudinal analyses from the German CF quality assurance (CFQA) project. Thorax *57*, 596–601. 10.1136/thorax.57.7.596.

13. Ashkenazi, M., Nathan, N., Sarouk, I., Aluma, B.E.B., Dagan, A., Bezalel, Y., Keler, S., Vilozni, D., and Efrati, O. (2019). Nutritional Status in Childhood as a Prognostic Factor in Patients with Cystic Fibrosis. Lung. 10.1007/s00408-019-00218-3.

14. Hayden, H.S., Eng, A., Pope, C.E., Brittnacher, M.J., Vo, A.T., Weiss, E.J., Hager, K.R., Martin, B.D., Leung, D.H., Heltshe, S.L., et al. (2020). Fecal dysbiosis in infants with cystic fibrosis is associated with early linear growth failure. Nat Med *26*, 215–221. 10.1038/s41591-019-0714-x.

15. Rogers, G.B., Carroll, M.P., Hoffman, L.R., Walker, A.W., Fine, D.A., and Bruce, K.D. (2010). Comparing the microbiota of the cystic fibrosis lung and human gut. Gut Microbes *1*, 85–93. 10.4161/gmic.1.2.11350.

16. Héry-arnaud, G., Boutin, S., Cuthbertson, L., Elborn, S.J., and Tunney, M.M. (2019). The lung and gut microbiome: what has to be taken into consideration for cystic fibrosis□? Journal of Cystic Fibrosis *18*, 13–21. 10.1016/j.jcf.2018.11.003.

17. Mahase, E. (2019). Cystic fibrosis: Triple therapy shows promising results. The BMJ *367*, 6347. 10.1136/bmj.l6347.

18. Collins, F.S. (2019). Realizing the Dream of Molecularly Targeted Therapies for Cystic Fibrosis. New England Journal of Medicine *381*, 1862–1863. 10.1056/nejme1912071.

19. Ooi, C.Y., Syed, S.A., Rossi, L., Garg, M., Needham, B., Avolio, J., Young, K., Surette, M.G., and Gonska, T. (2018). Impact of CFTR modulation with Ivacaftor on Gut Microbiota and Intestinal Inflammation. Sci Rep *8*, 1–8. 10.1038/s41598-018-36364-6.

20. Ronan, N.J., Einarsson, G.G., Deane, J., Fouhy, F., Rea, M., Hill, C., and Shanahan, F. (2022). Modulation , microbiota and inflammation in the adult CF gut□: A prospective study. Journal of Cystic Fibrosis. 10.1016/j.jcf.2022.06.002.

21. Pope, C.E., Vo, A.T., Hayden, H.S., Weiss, E.J., Durfey, S., Mcnamara, S., Ratjen, A., Grogan, B., Carter, S., Nay, L., et al. (2020). Changes in fecal microbiota with CFTR modulator therapy: A pilot study. Journal of Cystic Fibrosis. 10.1016/j.jcf.2020.12.002.

22. Harris, P.A., Taylor, R., Thielke, R., Payne, J., Gonzalez, N., and Conde, J.G. (2009). Research electronic data capture (REDCap)-A metadata-driven methodology and workflow process for providing translational research informatics support. J Biomed Inform *42*, 377–381. 10.1016/j.jbi.2008.08.010.

23. Reasoner, S.A., Fazili, I.F., Bernard, R., Parnell, J.M., Sokolow, A.G., Thomsen, K.F., Edwards, K.M., Brown, R.F., and Nicholson, M.R. (2022). Prevalence, Risk Factors, and Sequelae of Asymptomatic Clostridioides difficile Colonization in Children with Cystic Fibrosis. Journal of Cystic Fibrosis. 10.1016/j.jcf.2022.12.014.

24. Parnell, J.M., Fazili, I., Bloch, S.C., Lacy, D.B., Garcia-Lopez, V.A., Bernard, R., Skaar, E.P., Edwards, K.M., and Nicholson, M.R. (2021). Two-step Testing for Clostridioides Difficile is Inadequate in Differentiating Infection From Colonization in Children. J Pediatr Gastroenterol Nutr *72*, 378–383. 10.1097/MPG.0000000000002944.

25. Gaio, D., Anantanawat, K., To, J., Liu, M., Monahan, L., and Darling, A.E. (2022). Hackflex: Low-cost, high-throughput, Illumina Nextera Flex library construction. Microb Genom *8*. 10.1099/MGEN.0.000744.
26. Aronesty, E. (2011). ea-utils: Command-line tools for processing biological sequencing data. https://github.com/ExpressionAnalysis/ea-utils.
27. Blanco-Míguez, A., Beghini, F., Cumbo, F., McIver, L.J., Thompson, K.N., Zolfo, M., Manghi, P., Dubois, L., Huang, K.D., Thomas, A.M., et al. (2023). Extending and improving metagenomic taxonomic profiling with uncharacterized species using MetaPhlAn 4. Nat Biotechnol. 10.1038/s41587-023-01688-w.
28. Dixon, P. (2003). VEGAN, A Package of R Functions for Community Ecology. Journal of Vegetation Science *14*, 927–930.
29. Franzosa, E.A., McIver, L.J., Rahnavard, G., Thompson, L.R., Schirmer, M., Weingart, G., Lipson, K.S., Knight, R., Caporaso, J.G., Segata, N., et al. (2018). Species-level functional profiling of metagenomes and metatranscriptomes. Nat Methods *15*, 962–968. 10.1038/s41592-018-0176-y.
30. Caspi, R., Billington, R., Keseler, I.M., Kothari, A., Krummenacker, M., Midford, P.E., Ong, W.K., Paley, S., Subhraveti, P., and Karp, P.D. (2020). The MetaCyc database of metabolic pathways and enzymes-a 2019 update. Nucleic Acids Res *48*, D455–D453. 10.1093/nar/gkz862.
31. Abubucker, S., Segata, N., Goll, J., Schubert, A.M., Izard, J., Cantarel, B.L., Rodriguez-Mueller, B., Zucker, J., Thiagarajan, M., Henrissat, B., et al. (2012). Metabolic reconstruction for metagenomic data and its application to the human microbiome. PLoS Comput Biol *8*. 10.1371/journal.pcbi.1002358.
32. Kaminski, J., Gibson, M.K., Franzosa, E.A., Segata, N., Dantas, G., and Huttenhower, C. (2015). High-Specificity Targeted Functional Profiling in Microbial Communities with ShortBRED. PLoS Comput Biol *11*. 10.1371/journal.pcbi.1004557.
33. Jia, B., Raphenya, A.R., Alcock, B., Waglechner, N., Guo, P., Tsang, K.K., Lago, B.A., Dave, B.M., Pereira, S., Sharma, A.N., et al. (2017). CARD 2017: Expansion and model-centric curation of the comprehensive antibiotic resistance database. Nucleic Acids Res *45*, D566–D573. 10.1093/nar/gkw1004.
34. Gevers, D., Kugathasan, S., Denson, L.A., Vázquez-Baeza, Y., Van Treuren, W., Ren, B., Schwager, E., Knights, D., Song, S.J., Yassour, M., et al. (2014). The treatment-naive microbiome in new-onset Crohn's disease. Cell Host Microbe *15*, 382–392. 10.1016/j.chom.2014.02.005.
35. Enaud, R., Hooks, K.B., Barre, A., Barnetche, T., Hubert, C., Massot, M., Bazin, T., Clouzeau, H., Bui, S., Fayon, M., et al. (2019). Intestinal Inflammation in Children with Cystic Fibrosis Is Associated with Crohn's-Like Microbiota Disturbances. J Clin Med *8*, 645. 10.3390/jcm8050645.
36. Price, C.E., Hampton, T.H., Valls, R.A., Barrack, K.E., O'Toole, G.A., Madan, J.C., and Coker, M.O. (2023). Development of the intestinal microbiome in cystic fibrosis in early life. mSphere. 10.1128/msphere.00046-23.
37. Mallick, H., Rahnavard, A., McIver, L.J., Ma, S., Zhang, Y., Nguyen, L.H., Tickle, T.L., Weingart, G., Ren, B., Schwager, E.H., et al. (2021). Multivariable association discovery in population-scale meta-omics studies. PLoS Comput Biol *17*. 10.1371/journal.pcbi.1009442.

38. Salyers, A.A., Gupta, A., and Wang, Y. (2004). Human intestinal bacteria as reservoirs for antibiotic resistance genes. Trends Microbiol *12*, 412–416. 10.1016/j.tim.2004.07.004.
39. Wheatley, R.M., Caballero, J.D., van der Schalk, T.E., de Winter, F.H.R., Shaw, L.P., Kapel, N., Recanatini, C., Timbermont, L., Kluytmans, J., Esser, M., et al. (2022). Gut to lung translocation and antibiotic mediated selection shape the dynamics of Pseudomonas aeruginosa in an ICU patient. Nat Commun *13*, 6523. 10.1038/s41467-022-34101-2.
40. Rogers, G.B., Carroll, M.P., Hoffman, L.R., Walker, A.W., Fine, D.A., and Bruce, K.D. (2010). Comparing the microbiota of the cystic fibrosis lung and human gut. Gut Microbes *1*, 85–93. 10.4161/gmic.1.2.11350.
41. Green, H.D., and Jones, A.M. (2022). Managing Pulmonary Infection in Adults With Cystic Fibrosis: Adult Cystic Fibrosis Series. Chest *162*, 66–75. 10.1016/j.chest.2022.02.007.
42. Beghini, F., McIver, L.J., Blanco-Míguez, A., Dubois, L., Asnicar, F., Maharjan, S., Mailyan, A., Manghi, P., Scholz, M., Thomas, A.M., et al. (2021). Integrating taxonomic, functional, and strain-level profiling of diverse microbial communities with biobakery 3. Elife *10*. 10.7554/eLife.65088.
43. Mall, M.A., Brugha, R., Gartner, S., Legg, J., Moeller, A., Mondejar-Lopez, P., Prais, D., Pressler, T., Ratjen, F., Reix, P., et al. (2022). Efficacy and Safety of Elexacaftor/Tezacaftor/Ivacaftor in Children 6 Through 11 Years of Age with Cystic Fibrosis Heterozygous for F508del and a Minimal Function Mutation A Phase 3b, Randomized, Placebo-controlled Study. Am J Respir Crit Care Med *206*, 1361–1369. 10.1164/rccm.202202-0392OC.
44. Streibel, C., Willers, C.C., Pusterla, O., Bauman, G., Stranzinger, E., Brabandt, B., Bieri, O., Curdy, M., Bullo, M., Frauchiger, B.S., et al. (2023). Effects of elexacaftor/tezacaftor/ivacaftor therapy in children with cystic fibrosis – a comprehensive assessment using lung clearance index, spirometry, and functional and structural lung MRI. Journal of Cystic Fibrosis. 10.1016/j.jcf.2022.12.012.
45. Jordan, K.D., Zemanick, E.T., Taylor-Cousar, J.L., and Hoppe, J.E. (2023). Managing cystic fibrosis in children aged 6-11yrs: a critical review of elexacaftor/tezacaftor/ivacaftor combination therapy. Expert Rev Respir Med. 10.1080/17476348.2023.2179989.
46. Kapouni, N., Moustaki, M., Douros, K., and Loukou, I. (2023). Efficacy and Safety of Elexacaftor-Tezacaftor-Ivacaftor in the Treatment of Cystic Fibrosis: A Systematic Review. Children *10*, 554. 10.3390/children10030554.
47. Wainwright, C., McColley, S.A., McNally, P., Powers, M., Ratjen, F., Rayment, J.H., Retsch-Bogart, G., Roesch, E., Ahluwalia, N., Chin, A., et al. (2023). Long-Term Safety and Efficacy of Elexacaftor/Tezacaftor/Ivacaftor in Children Aged ≥6 Years with Cystic Fibrosis and At Least One F508del Allele: A Phase 3, Open-Label Clinical Trial. Am J Respir Crit Care Med. 10.1164/rccm.202301-0021OC.
48. Cornet, M., Robin, G., Ciciriello, F., Bihouee, T., Marguet, C., Roy, V., Lebourgeois, M., Chedevergne, F., Bonnel, A.S., Kelly, M., et al. (2022). Profiling the response to lumacaftor-ivacaftor in children with cystic between fibrosis and new insight from a French-Italian real-life cohort. Pediatr Pulmonol. 10.1002/ppul.26123.
49. Antosca, K.M., Chernikova, D.A., Ruoff, K.L., Li, K., Guill, M.F., MacKenzie, T.A., Dorman, D.B., Moulton, L.A., Williams, M.A., Aldrich, B.J., et al. (2019). Altered Stool

Microbiota of Infants with Cystic Fibrosis Shows Reduction in Genera Associated with Immune Programming. J Bacteriol *201*, 1–15. 10.1101/342782.

50. Kristensen, M., Prevaes, S.M.P.J., Kalkman, G., Tramper-Stranders, G.A., Hasrat, R., de Winter- de Groot, K.M., Janssens, H.M., Tiddens, H.A., van Westreenen, M., Sanders, E.A.M., et al. (2020). Development of the gut microbiota in early life: The impact of cystic fibrosis and antibiotic treatment. Journal of Cystic Fibrosis *19*, 553–561. 10.1016/j.jcf.2020.04.007.

51. Salerno, P., Verster, A.J., Valls, R.A., Barrack, K.E., Price, C.E., Madan, J.C., O'Toole, G.A., and Ross, B.D. (2023). Persistent delay in maturation of the developing gut microbiota in infants with cystic fibrosis. bioRxiv. 10.1101/2023.05.02.539134.

52. Matamouros, S., Hayden, H.S., Hager, K.R., Brittnacher, M.J., Lachance, K., Weiss, E.J., Pope, C.E., Imhaus, A.F., McNally, C.P., Borenstein, E., et al. (2018). Adaptation of commensal proliferating Escherichia coli to the intestinal tract of young children with cystic fibrosis. Proc Natl Acad Sci U S A *115*, 1605–1610. 10.1073/pnas.1714373115.

53. Hoffman, L.R., Pope, C.E., Hayden, H.S., Heltshe, S., Levy, R., McNamara, S., Jacobs, M.A., Rohmer, L., Radey, M., Ramsey, B.W., et al. (2014). Escherichia coli dysbiosis correlates with gastrointestinal dysfunction in children with cystic fibrosis. Clinical Infectious Diseases *58*, 396–399. 10.1093/cid/cit715.

54. Dhaliwal, J., Leach, S., Katz, T., Nahidi, L., Pang, T., Lee, J.M., Strachan, R., Day, A.S., Jaffe, A., and Ooi, C.Y. (2015). Intestinal inflammation and impact on growth in children with cystic fibrosis. J Pediatr Gastroenterol Nutr *60*, 521–526. 10.1097/MPG.0000000000000683.

55. Coffey, M.J., Nielsen, S., Wemheuer, B., Kaakoush, N.O., Garg, M., Needham, B., Pickford, R., Ja, A., Thomas, T., and Chee Y. Ooi (2019). Gut Microbiota in Children With Cystic Fibrosis: A Taxonomic and Functional Dysbiosis. Sci Rep *9*, 1–14. 10.1038/s41598-019-55028-7.

56. Yamada, A., Komaki, Y., Komaki, F., Micic, D., Zullow, S., and Sakuraba, A. (2018). Risk of gastrointestinal cancers in patients with cystic fibrosis: a systematic review and meta-analysis. Lancet Oncol *19*, 758–767. 10.1016/S1470-2045(18)30188-8.

57. Garg, M., Leach, S.T., Coffey, M.J., Katz, T., Strachan, R., Pang, T., Needham, B., Lui, K., Ali, F., Day, A.S., et al. (2017). Age-dependent variation of fecal calprotectin in cystic fibrosis and healthy children. Journal of Cystic Fibrosis *16*, 631–636. 10.1016/j.jcf.2017.03.010.

58. Rumman, N., Sultan, M., El-Chammas, K., Goh, V., Salzman, N., Quintero, D., and Werlin, S. (2014). Calprotectin in Cystic Fibrosis. BMC Pediatr *14*. 10.1186/1471-2431-14-133.

59. Beaufils, F., Mas, E., Mittaine, M., Addra, M., Fayon, M., Delhaes, L., Clouzeau, H., Galode, F., Lamireau, T., Bui, S., et al. (2020). Increased Fecal Calprotectin Is Associated with Worse Gastrointestinal Symptoms and Quality of Life Scores in Children with Cystic Fibrosis. J Clin Med *9*, 4080. 10.3390/jcm9124080.

60. Schwarzenberg, S.J., Vu, P.T., Skalland, M., Hoffman, L.R., Pope, C., Gelfond, D., Narkewicz, M.R., Nichols, D.P., Heltshe, S.L., Donaldson, S.H., et al. (2022). Elexacaftor/tezacaftor/ivacaftor and gastrointestinal outcomes in cystic fibrosis: Report of promise-GI. Journal of Cystic Fibrosis. 10.1016/j.jcf.2022.10.003.

61. Baldwin-Hunter, B.L., Rozenberg, F.D., Annavajhala, M.K., Park, H., DiMango, E.A., Keating, C.L., Uhlemann, A.-C., and Abrams, J.A. (2023). The gut microbiome, short

chain fatty acids, and related metabolites in cystic fibrosis patients with and without colonic adenomas. Journal of Cystic Fibrosis. 10.1016/j.jcf.2023.01.013.

62. Miragoli, F., Federici, S., Ferrari, S., Minuti, A., Rebecchi, A., Bruzzese, E., Buccigrossi, V., Guarino, A., and Callegari, M.L. (2017). Impact of cystic fibrosis disease on archaea and bacteria composition of gut microbiota. FEMS Microbiol Ecol *93*. 10.1093/femsec/fiw230.

63. Burke, D.G., Fouhy, F., Harrison, M.J., Rea, M.C., Cotter, P.D., O'Sullivan, O., Stanton, C., Hill, C., Shanahan, F., Plant, B.J., et al. (2017). The altered gut microbiota in adults with cystic fibrosis. BMC Microbiol *17*, 1–11. 10.1186/s12866-017-0968-8.

64. Rivera-Chávez, F., Lopez, C.A., and Bäumler, A.J. (2017). Oxygen as a driver of gut dysbiosis. Free Radic Biol Med *105*, 93–101. 10.1016/j.freeradbiomed.2016.09.022.

65. Shah, Y.M. (2016). The role of hypoxia in intestinal inflammation. Mol Cell Pediatr *3*. 10.1186/s40348-016-0030-1.

66. Rigottier-Gois, L. (2013). Dysbiosis in inflammatory bowel diseases: The oxygen hypothesis. ISME Journal *7*, 1256–1261. 10.1038/ismej.2013.80.

67. López-Causapé, C., Rojo-Molinero, E., MacIà, M.D., and Oliver, A. (2015). The problems of antibiotic resistance in cystic fibrosis and solutions. Expert Rev Respir Med *9*, 73–88. 10.1586/17476348.2015.995640.

68. Taylor, S.L., Leong, L.E.X., Sims, S.K., Keating, R.L., Papanicolas, L.E., Richard, A., Mobegi, F.M., Wesselingh, S., Burr, L.D., and Rogers, G.B. (2021). The cystic fibrosis gut as a potential source of multidrug resistant pathogens. Journal of Cystic Fibrosis *20*, 413–420. 10.1016/j.jcf.2020.11.009.

69. Patel, D., Mathews, S., van Unen, V., Chan, J.E., Al-Hammadi, N., Borowitz, D., Gelfond, D., and Sellers, Z.M. (2022). Impaired distal colonic pH in adults with cystic fibrosis. Journal of Cystic Fibrosis. 10.1016/j.jcf.2022.12.011.

70. Gelfond, D., Heltshe, S., Ma, C., Rowe, S.M., Frederick, C., Uluer, A., Sicilian, L., Konstan, M., Tullis, E., Roach, R.N.C., et al. (2017). Impact of CFTR modulation on intestinal pH, motility, and clinical outcomes in patients with cystic fibrosis and the G551D mutation. Clin Transl Gastroenterol *8*. 10.1038/ctg.2017.10.

TABLES AND FIGURES

Table 1. Cohort Baseline Details

Figure 1. Study Schematic, Timeline, and Clinical Improvement after ELX/TEZ/IVA

Figure 2. Microbiome Diversity and Intestinal Carriage of Antibiotic Resistance Genes

Figure 3. Specific Microbial Taxonomic Changes after ELX/TEZ/IVA

Figure 4. Intestinal Inflammation Decreases after ELX/TEZ/IVA and Microbiome Functional Changes

Supplementary Figure 1. Clinical Data Across the Four-Timepoints

Supplementary Figure 2. Microbiome Beta Diversity

Supplementary Figure 3. Reduced Abundance of Intestinal Antibiotic Resistance Genes

Supplementary Figure 4. Respiratory Taxa in Stool Samples

Supplementary Figure 5. Fecal Calprotectin at Four-Timepoints and Differentially Abundant KEGG Orthology Groups

Supplementary Table S1. Complete Metadata

Supplementary Table S2. Species MaAsLin2 Results

Supplementary Table S3. Differentially Abundant Species with Respect to ELX/TEZ/IVA

Supplementary Table S4. MaAsLin2 Results Across Taxonomic Levels

Supplementary Table S5. MaAsLin2 Results of Antibiotic Resistance Genes

Supplementary Table S6. MaAsLin2 Results of KEGG Orthology Groups

Supplementary Table S7. Differentially Abundant KEGG Orthology Groups with Respect to ELX/TEZ/IVA

Supplementary Table S8. MaAsLin2 Results of MetaCyc Pathways

Supplementary Table S9. Differentially Abundant MetaCyc Pathways with Respect to ELX/TEZ/IVA

Supplementary Dataset 1. Compiled Metadata and Metagenomic Results

FIGURE LEGENDS

Figure 1. Study Schematic, Timeline, and Clinical Improvement after ELX/TEZ/IVA.
A) Overview of study procedure and analyses. **B)** Timeline illustrating the four timepoints. Day 0 is depicted as the day of ELX/TEZ/IVA initiation. A total of 114 samples were collected from 39 unique patients, of which 53 samples were before ELX/TEZ/IVA treatment and 61 samples after treatment. **C-E)** Depictions of clinical data before and after ELX/TEZ/IVA; **(C)** ppFEV1, **(D)** BMI percentile, **(E)** antibiotic days per 6-months. Each dot represents the clinical data associated with a stool sample. P values calculated by Wilcoxon rank-sum test.

Figure 2. Microbiome Diversity and Intestinal Carriage of Antibiotic Resistance Genes.
A and B) Alpha diversity before and after ELX/TEZ/IVA. Shannon Index calculated with the R package vegan using species abundance table from Metaphlan4. Microbial richness represents the number of unique species per sample. Each dot represents a stool sample (n=114). P values calculated by Wilcoxon rank-sum test. **C and D)** Alpha diversity between samples with and without recent antibiotic exposure. Recent antibiotic exposure categorized as any systemic antibiotic within the past 6-months. Shannon Index calculated with the R package vegan using species abundance table from MetaPhlAn4. Microbial richness represents the number of unique species per sample. Each dot represents a stool sample (n=114). P values calculated by

Wilcoxon rank-sum test. **E)** Antibiotic resistance gene **(**ARG) abundance (RPKM) before and after ELX/TEZ/IVA. ARGs were profiled using ShortBRED and the Comprehensive Antibiotic Resistance Database (CARD). Each dot represents a stool sample (n=114). P values calculated by Wilcoxon rank-sum test. **F)** ARG abundance (RPKM) by class of antibiotic to which they confer resistance. Abundance values of zero are plotted on the vertical axis. P values calculated by Wilcoxon signed-rank test.

Figure 3. Specific Microbial Taxonomic Changes after ELX/TEZ/IVA.
A) Differentially abundant species before and after ELX/TEZ/IVA. The results are depicted with significance (−log10 of the FDR) (Y axis) *vs*. log2(FoldChange). MaAsLin2 multivariable association modeling was implemented in R, using ELX/TEZ/IVA status, age, and recent antibiotics as fixed effects in the model. Participant ID was used as a random effect. Horizontal dashed line depicts FDR=0.1. Species reaching statistical significance (FDR≤0.10) are highlighted in solid colors whereas other species are gray. **B)** Species of interest from differential abundance testing before and after ELX/TEZ/IVA. MaAsLin2 FDR is depicted.

Figure 4. Intestinal Inflammation Decreases after ELX/TEZ/IVA and Microbiome Functional Changes. A) Fecal calprotectin before and after ELX/TEZ/IVA. Each dot represents a stool sample (n=114). P values calculated by Wilcoxon rank-sum test. **B-C)** Microbial dysbiosis index (MDI) before and after ELX/TEZ/IVA **(B)** or between samples with and without recent antibiotic exposure **(C)**. MDI calculated as the log10 ratio of species positively/negatively correlated with new onset pediatric Crohn's disease[34]. Each dot represents a stool sample (n=114). P values calculated by Wilcoxon rank-sum test. **D)** Differentially abundant KEGG orthologs following MaAsLin2 multivariable association modeling, using ELX/TEZ/IVA status, age, and recent antibiotics as fixed effects in the model. Participant ID was used as a random effect. Horizontal dashed line depicts FDR=0.25. **E)** Subset of differentially abundant MetaCyc pathways following MaAsLin2 multivariable association modeling, using ELX/TEZ/IVA status, age, and recent antibiotics as fixed effects in the model. Only pathways with FDR<0.25 are depicted.

Supplementary Figure S1. A-D) Clinical metadata *vs.* timepoint; **(A)** ppFEV1, **(B)** BMI percentile, **(C)** weight percentile, and **(D)** height percentile. Each dot represents the clinical data associated with a stool sample. Red line indicates the mean, and gray lines represent individual patients. P values calculated by Wilcoxon signed-rank test.

Supplementary Figure S2. A-B) Alpha diversity *vs*. timepoint. Shannon Index (**A**) calculated with the R package vegan using species abundance table from Metaphlan4. Microbial richness (**B**) represents the number of unique species per sample. Each dot represents a stool sample (n=114). P values calculated by Wilcoxon signed-rank test. **C)** Principal component analysis of Bray-Curtis distances before and after ELX/TEZ/IVA. Bray-Curtis distance matrix computed with vegan. PERMANOVA and PERMDISP computed by the vegan package with the functions adonis2 and betadisp, respectively. Ellipse depicts the 95% confidence level. **D)** Principal component analysis of weighted UniFrac distances before and after ELX/TEZ/IVA. Weighted UniFrac computed with MetaPhlAn4 R script. PERMANOVA and PERMDISP computed by the vegan package with the functions adonis2 and betadisp, respectively. Ellipse depicts the 95% confidence level. **E)** Principal component analysis of the Bray-Curtis distances between samples with and without recent antibiotic exposure. Distance matrix generated by the R package vegan using the MetaPhlAn4 species table. PERMANOVA and PERMDISP computed in vegan with the functions adonis2 and betadisp, respectively. Ellipse depicts the 95% confidence level.

Supplementary Figure S3. A) Cumulative antibiotic days per 6-months prior to stool sample collection. P values calculated by Wilcoxon signed-rank test. **B)** ARG richness (unique genes) before and after ELX/TEZ/IVA. ARGs were profiled using ShortBRED and the Comprehensive Antibiotic Resistance Database (CARD). Each dot represents a stool sample (n=114). P values calculated by Wilcoxon rank-sum test. **C)** Cumulative relative abundance (RPKM) of ARGs conferring resistance to peptide antibiotics. P values calculated by Wilcoxon rank-sum test. **D)** Relative abundance (RPKM) of the most prevalent ARGs conferring resistance to peptide antibiotics. MaAsLin2 FDR is depicted. **E)** Cumulative relative abundance (RPKM) of ARGs conferring resistance to other antibiotics. P values calculated by Wilcoxon rank-sum test. **F)** Relative abundance (RPKM) of the most prevalent ARGs conferring resistance to other antibiotics. MaAsLin2 FDR is depicted.

Supplementary Figure S4. A) *Roseburia faecis* relative abundance between samples with and without recent antibiotic exposure. Each dot represents a stool sample (n=114). MaAsLin2 FDR is depicted. **B)** Relative abundance of respiratory genera in stool samples before and after ELX/TEZ/IVA. Each dot represents a stool sample (n=114). MaAsLin2 FDR is depicted.

Supplementary Figure S5. A) Fecal calprotectin (μg/g) *vs*. study timepoint. Red line indicates the mean, and gray lines represent individual patients. P values calculated by Wilcoxon signed-rank test. **B)** Differentially abundant oxidative phosphorylation KEGG orthology (KO) groups from MaAsLin2 (FDR<0.25). Groups correspond to red points in Figure 5A. log2(FoldChange), which is equivalent to MaAsLin2 coefficient, is depicted. **C)** Taxonomic stratification of differentially abundant oxidative phosphorylation KO groups. KO groups correspond to groups in panel A.

Participants (*n*)	39
Median age (yrs) at ELX/TEZ/IVA Initiation (IQR)	9.86 (8.87, 12.15)
6-11 years	65.8%
12-18 years	34.2%
Sex	
Male sex	56.4%
Female sex	43.6%
CFTR Genotype	
Phe508del/Phe508del	53.8%
Phe508del/Other	46.2%
Prior CFTR Modulator Therapy	35.9%
TEZ/IVA	9
LUM/IVA	4
IVA	1
Comorbidities	
Pancreatic insufficiency	100%
CFLD	20.5%
CFRD	7.7%
Respiratory Culture History	
Methicillin-resistant *Staphylococcus aureus*	51.3%
Pseudomonas aeruginosa	35.9%
Stenotrophomonas maltophilia	28.2%
Nontuberculous *Mycobacteria*	2.6%
Burkholderia spp.	0%

Table 1. Cohort Details. Table includes patient characteristics at the time of recruitment prior to initiation of ELX/TEZ/IVA. Categorical and dichotomous variables are expressed as *n* and as a proportion of the total for the group. Respiratory culture history refers to isolation of the microbial species from sputum or bronchoalveolar lavage within the 3 years prior to enrollment. Abbreviations: IQR (interquartile range); CFLD (CF-related liver disease); CFRD (CF-related diabetes); TEZ/IVA (Tezacaftor/ivacaftor, Symdeko™); LUM/IVA (Lumacaftor/ivacaftor, Orkambi™); and IVA (Ivacaftor, Kalydeco™).

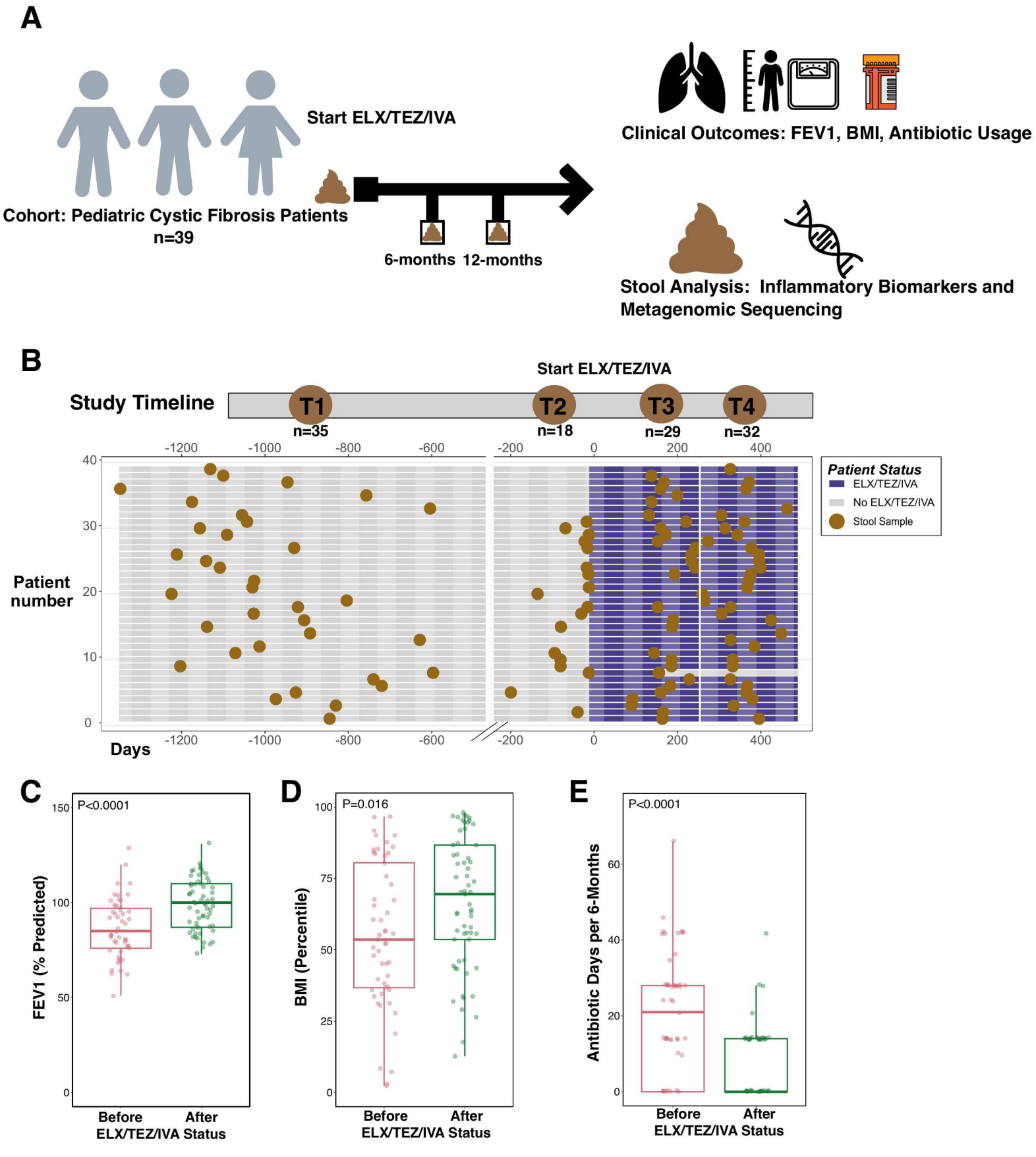
A
Start ELX/TEZ/IVA
Cohort: Pediatric Cystic Fibrosis Patients
n=39
6-months
12-months
Clinical Outcomes: FEV1, BMI, Antibiotic Usage
Stool Analysis: Inflammatory Biomarkers and Metagenomic Sequencing
B
Start ELX/TEZ/IVA
Study Timeline
T1
T2
T3
T4
n=35
n=18
n=29
n=32
Patient number
Days
Patient Status
ELX/TEZ/IVA
No ELX/TEZ/IVA
Stool Sample
C
P<0.0001
FEV1 (% Predicted)
Before
After
ELX/TEZ/IVA Status
D
P=0.016
BMI (Percentile)
Before
After
ELX/TEZ/IVA Status
E
P<0.0001
Antibiotic Days per 6-Months
Before
After
ELX/TEZ/IVA Status

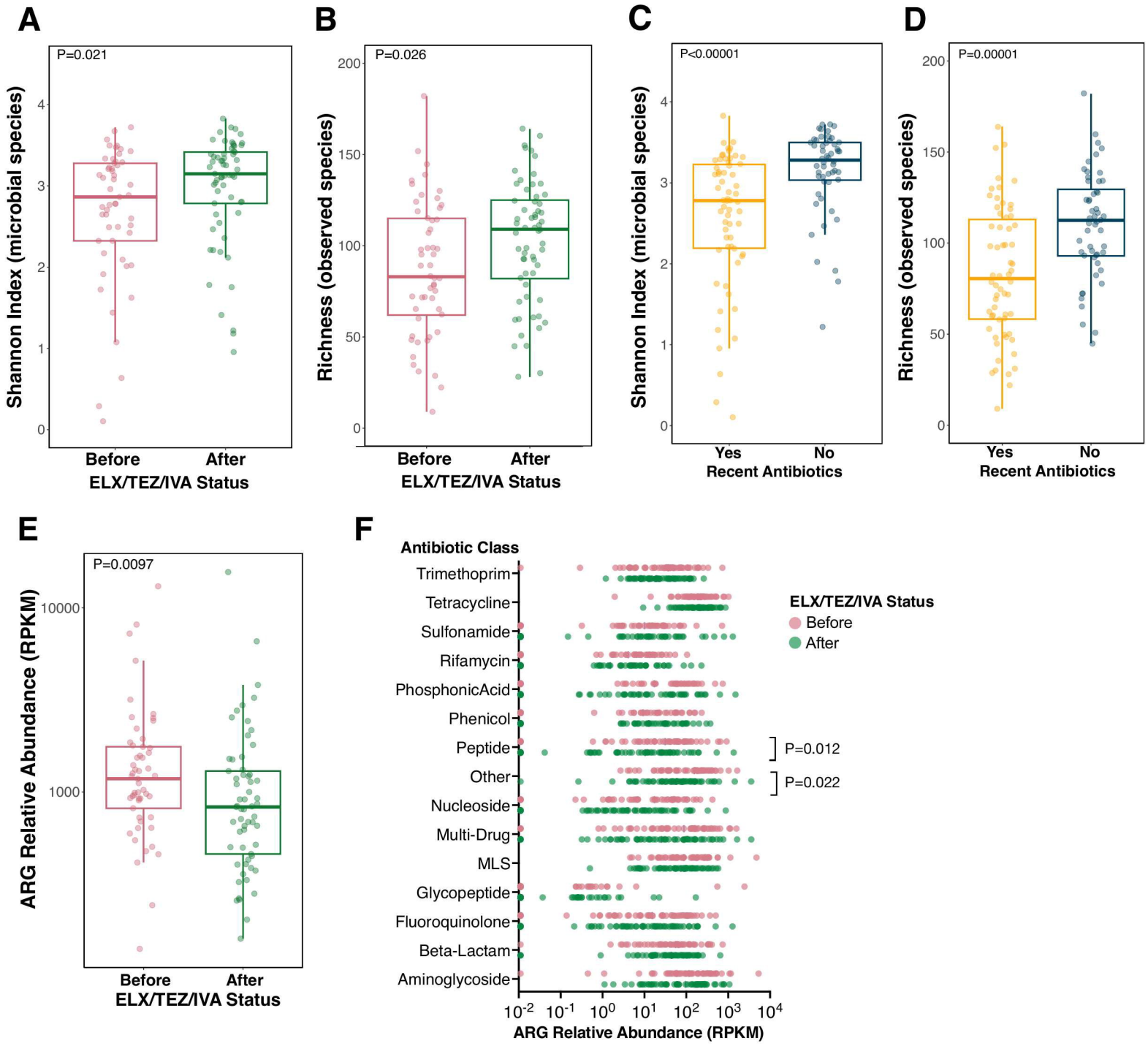
A
P=0.021
Shannon Index (microbial species)
Before
After
ELX/TEZ/IVA Status
B
P=0.026
Richness (observed species)
Before
After
ELX/TEZ/IVA Status
C
P<0.00001
Shannon Index (microbial species)
Yes
No
Recent Antibiotics
D
P=0.00001
Richness (observed species)
Yes
No
Recent Antibiotics
E
P=0.0097
ARG Relative Abundance (RPKM)
Before
After
ELX/TEZ/IVA Status
F
Antibiotic Class
Trimethoprim
Tetracycline
Sulfonamide
Rifamycin
PhosphonicAcid
Phenicol
Peptide
Other
Nucleoside
Multi-Drug
MLS
Glycopeptide
Fluoroquinolone
Beta-Lactam
Aminoglycoside
P=0.012
P=0.022
ELX/TEZ/IVA Status
Before
After
ARG Relative Abundance (RPKM)

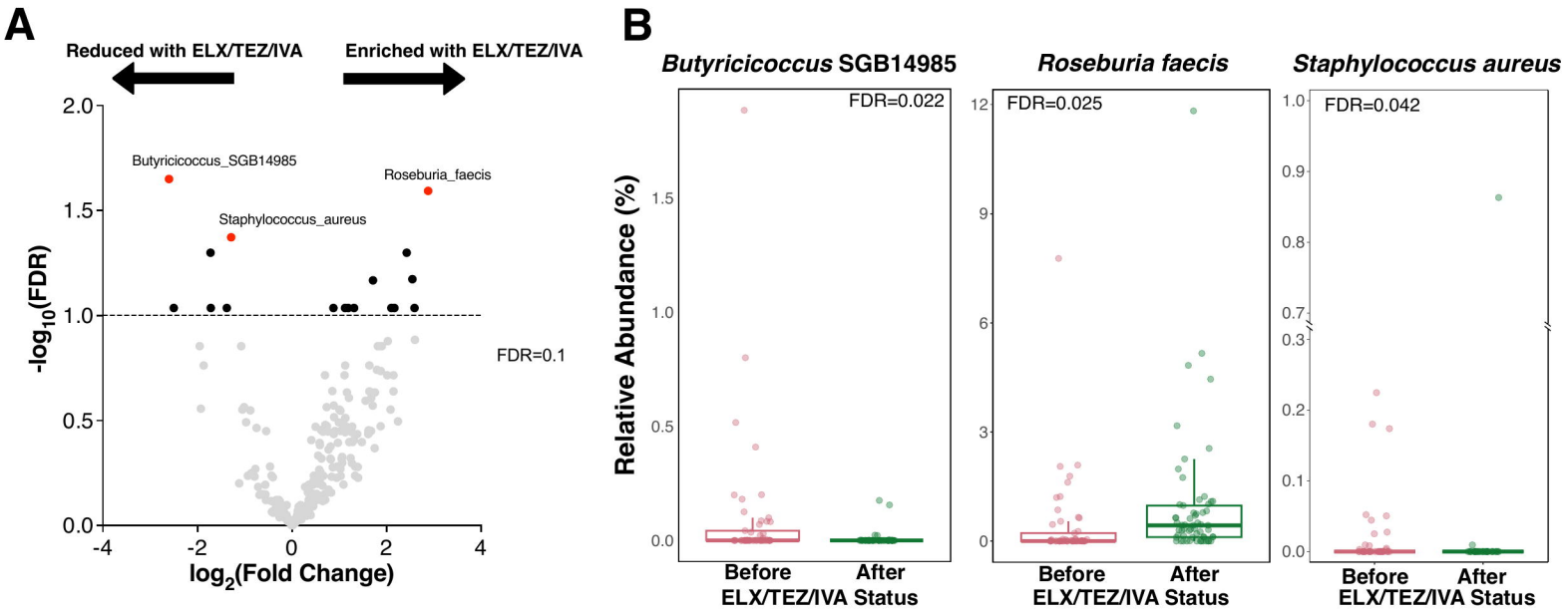
A
Reduced with ELX/TEZ/IVA
Enriched with ELX/TEZ/IVA
Butyricicoccus_SGB14985
Roseburia_faecis
Staphylococcus_aureus
FDR=0.1
-log10(FDR)
log2(Fold Change)
B
Butyricicoccus SGB14985
Roseburia faecis
Staphylococcus aureus
FDR=0.022
FDR=0.025
FDR=0.042
Relative Abundance (%)
Before
After
ELX/TEZ/IVA Status

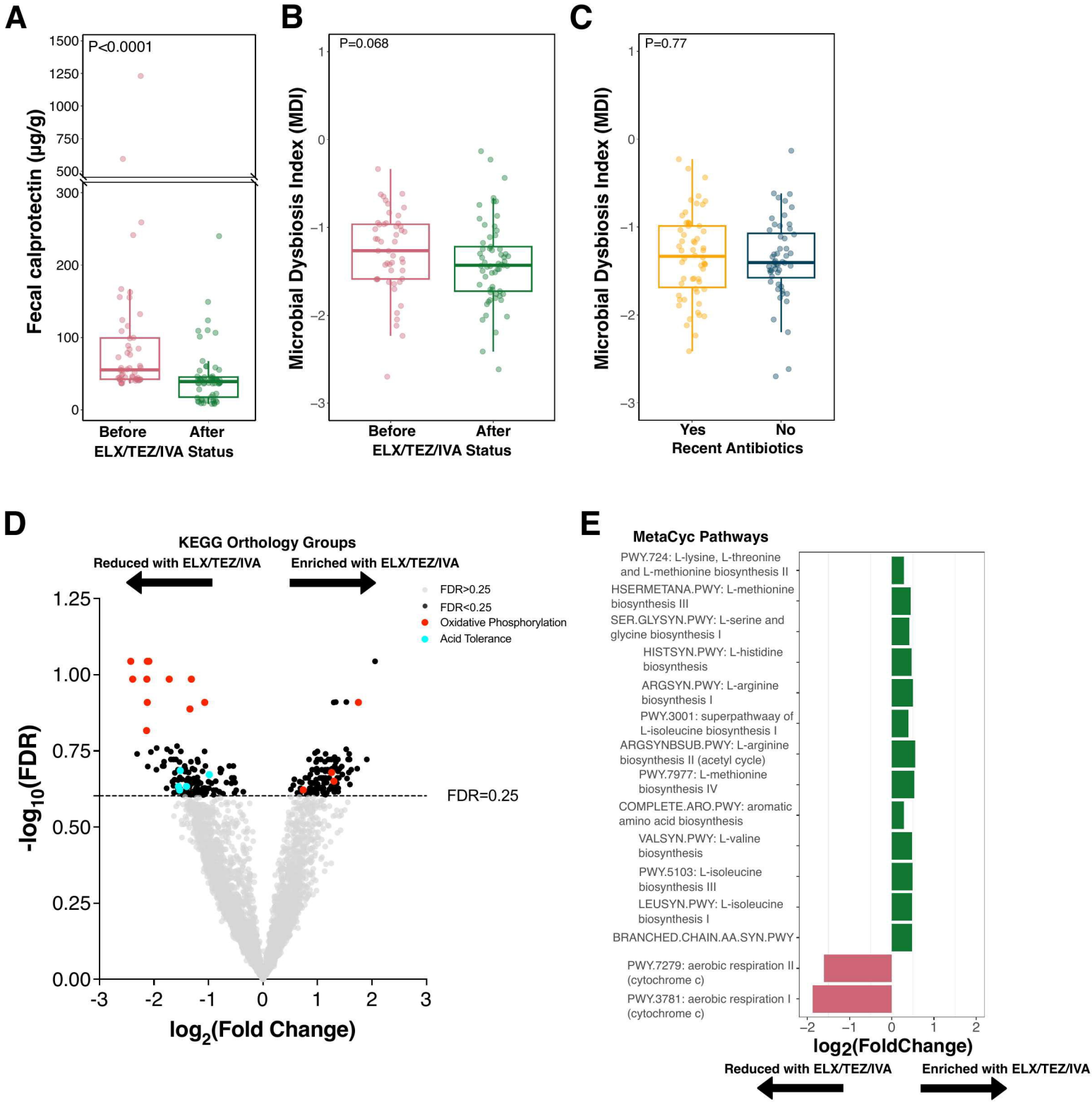
A
P<0.0001
Fecal calprotectin (µg/g)
1500
1250
1000
750
500
300
200
100
0
Before
After
ELX/TEZ/IVA Status
B
P=0.068
Microbial Dysbiosis Index (MDI)
1
0
−1
−2
−3
Before
After
ELX/TEZ/IVA Status
C
P=0.77
Microbial Dysbiosis Index (MDI)
1
0
−1
−2
−3
Yes
No
Recent Antibiotics
D
KEGG Orthology Groups
Reduced with ELX/TEZ/IVA
Enriched with ELX/TEZ/IVA
FDR>0.25
FDR<0.25
Oxidative Phosphorylation
Acid Tolerance
FDR=0.25
-log10(FDR)
1.25
1.00
0.75
0.50
0.25
0.00
-3
-2
-1
0
1
2
3
log2(Fold Change)
E
MetaCyc Pathways
PWY.724: L-lysine, L-threonine and L-methionine biosynthesis II
HSERMETANA.PWY: L-methionine biosynthesis III
SER.GLYSYN.PWY: L-serine and glycine biosynthesis I
HISTSYN.PWY: L-histidine biosynthesis
ARGSYN.PWY: L-arginine biosynthesis I
PWY.3001: superpathwaay of L-isoleucine biosynthesis I
ARGSYNBSUB.PWY: L-arginine biosynthesis II (acetyl cycle)
PWY.7977: L-methionine biosynthesis IV
COMPLETE.ARO.PWY: aromatic amino acid biosynthesis
VALSYN.PWY: L-valine biosynthesis
PWY.5103: L-isoleucine biosynthesis III
LEUSYN.PWY: L-isoleucine biosynthesis I
BRANCHED.CHAIN.AA.SYN.PWY
PWY.7279: aerobic respiration II (cytochrome c)
PWY.3781: aerobic respiration I (cytochrome c)
−2
−1
0
1
2
log2(FoldChange)
Reduced with ELX/TEZ/IVA
Enriched with ELX/TEZ/IVA

Supplemental Figure 1

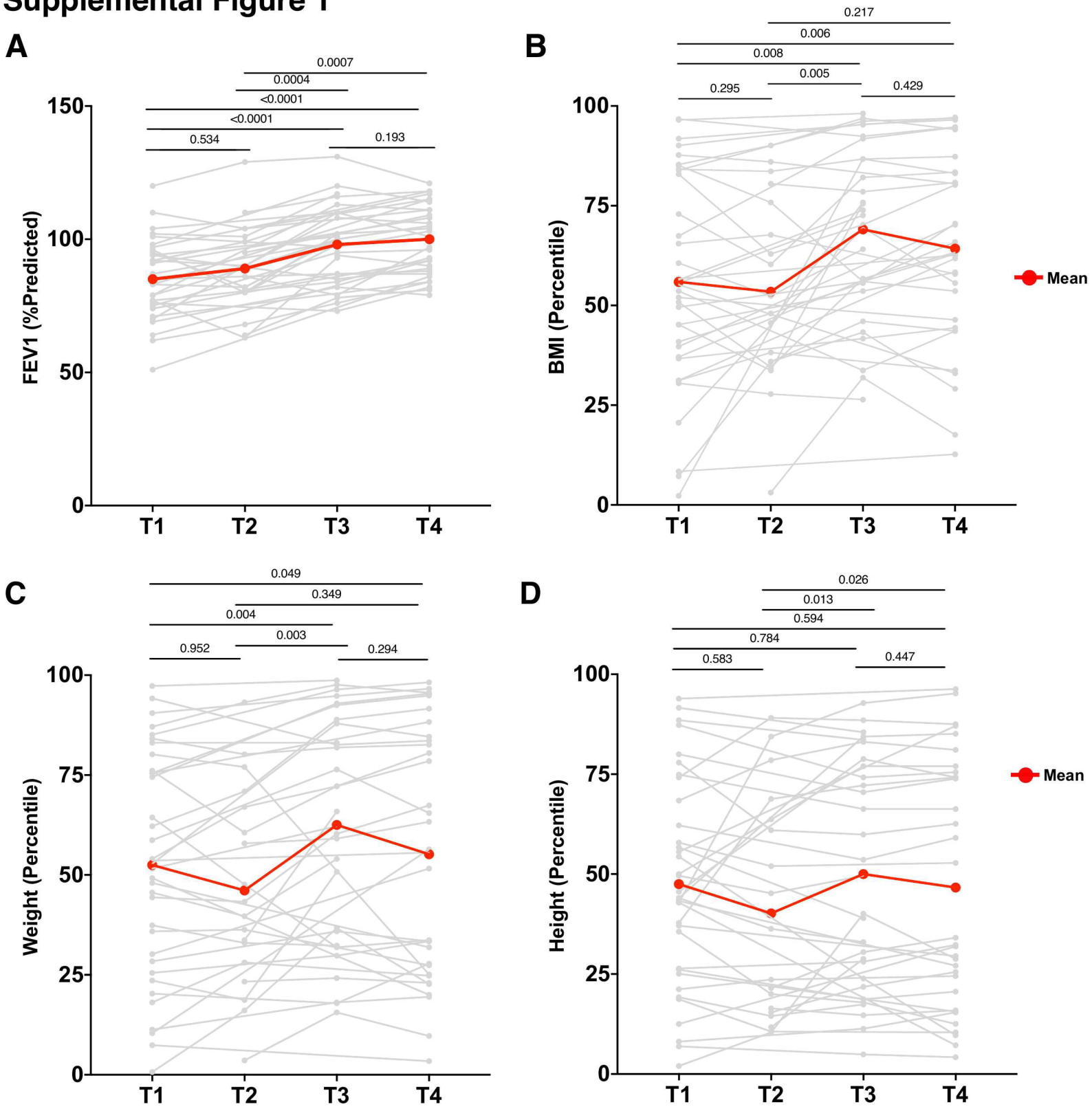

Supplemental Figure 2

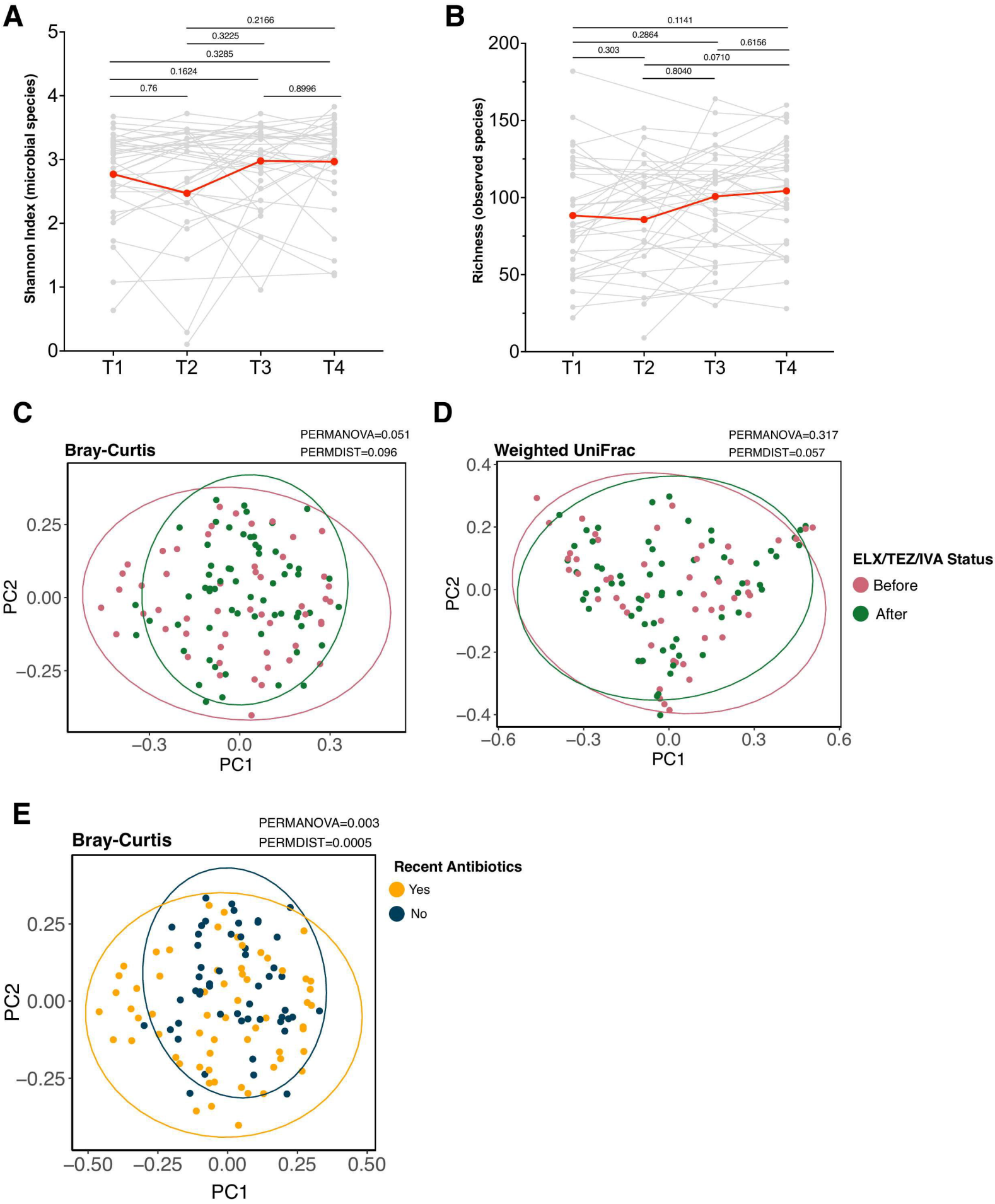

Supplemental Figure 3

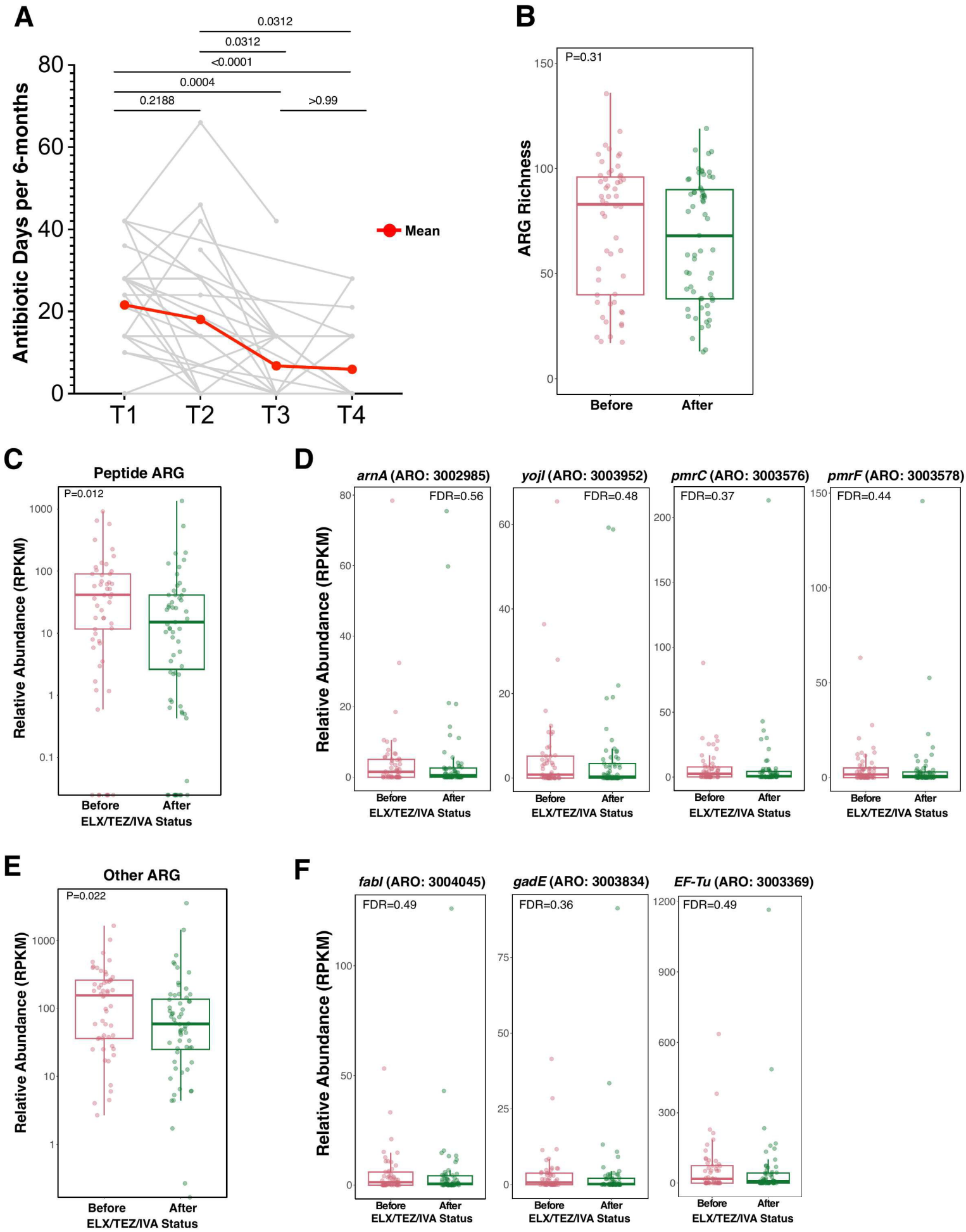

Supplemental Figure 4

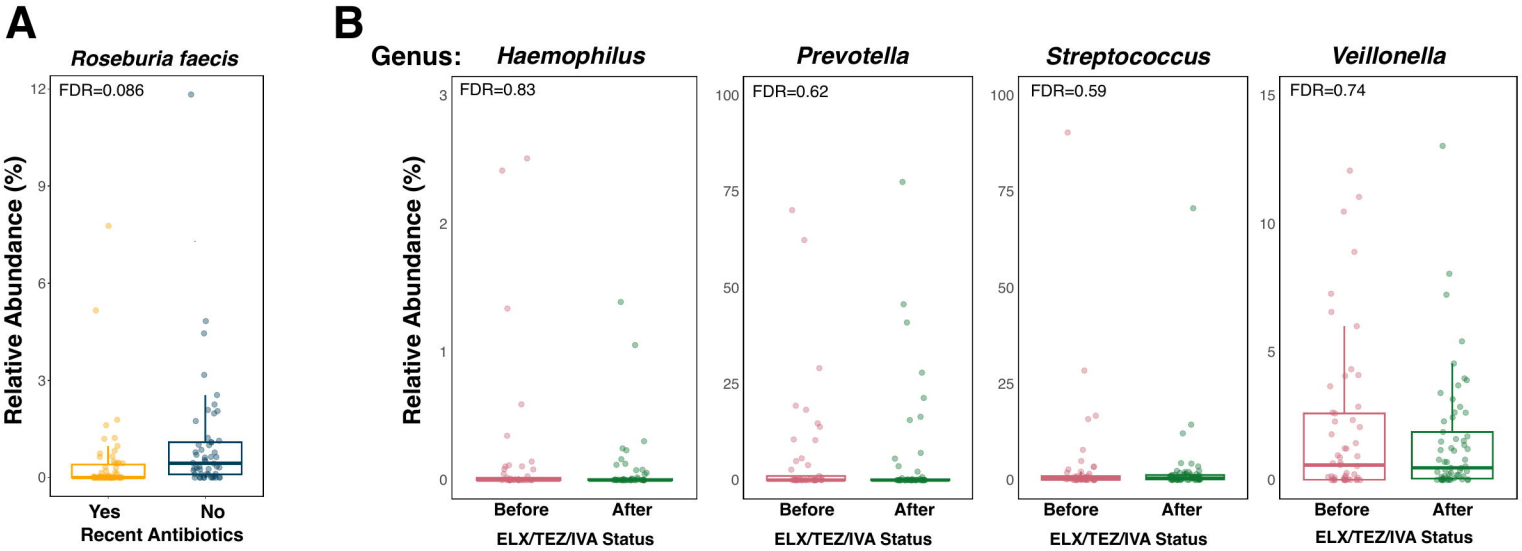
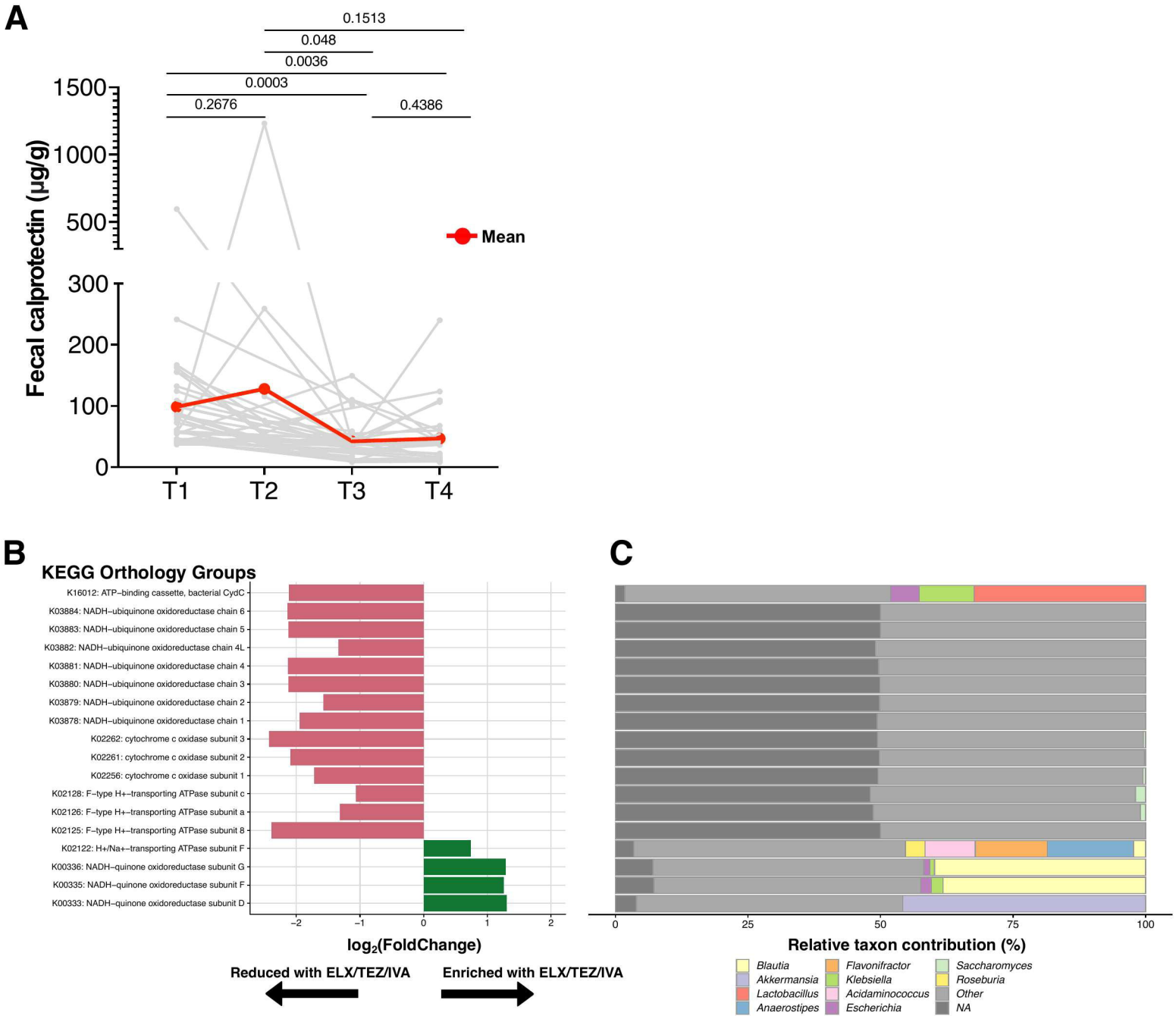
Supplemental Figure 5